

A REVIEW OF THE INVESTIGATIONS OF THE FLEISCHMANN-PONS PHENOMENA

JOHN O'M. BOCKRIS, GUANG H. LIN, and NIGEL J. C. PACKHAM
Texas A&M University, Department of Chemistry
Surface Electrochemistry Laboratory, College Station, Texas 77843

OVERVIEW

COLD FUSION

KEYWORDS: cold fusion, electrolysis, radiation, tritium, neutrons

Received March 26, 1990

Accepted for Publication April 19, 1990

A review of the recent investigations of the Fleischmann-Pons effect ("cold fusion") is given. A discussion of the proposed theories and models to account for the observations is also given. Suggestions for future research in this area are discussed.

INTRODUCTION

On March 23, 1989, Fleischmann and Pons¹ and Jones et al.² reported the observation of anomalous products during constant-current electrolysis of D₂O on palladium. Specifically, they reported production of excess heat, tritium, neutrons, and gamma rays.

Since that time, research has been performed throughout the world in an attempt to reproduce and confirm these claims. There has been widespread disappointment in that the phenomena cannot be switched on and confirmed in a simple way. Even those with electrochemical experience and plentiful resources (such as those at national laboratories) have reported negatively on the grounds that phenomena were visible only in sporadic bursts and "nothing consistent" could be measured. This sporadic nature of the effects, with periods of weeks in which observers do not record the phenomena reported by Fleischmann and Pons, remains a marked difficulty.^a

TYPICAL CELLS

Most research into nuclear electrochemical phenomena uses cells in which the electrode pretreatment and solution types are varied. The cell described in

^aConversely, there are already claims as to techniques that lead to an immediate switch-on.

Ref. 1, typical of the generally accepted cell design (Fig. 1), was a double-walled glass cell containing the electrochemical apparatus and monitoring equipment, e.g., temperature probes. The electrolytic solution was 0.1 M LiOD in D₂O. The electrodes were a cathode of palladium (1- to 6-mm diam) with an anode of platinum wire wrapped around it, separated by glass rods. In some designs, a catalyst for the recombination of the evolved gases (D₂ and O₂) was included either inside or outside the cell. Constant-current electrolysis was performed for periods of time varying from tens of hours to six months, with the current density ranging between 10 and 1000 mA/cm². The cell was calibrated by a joule heater supplying nonelectrochemical heat to the cell, the temperature difference ΔT between the inside of the cell and a water bath being measured (Fig. 2). The current was then turned on and the ΔT (and the corresponding power-out W_{out}) was compared with that expected for the heat on the grounds of thermochemical reasoning. If the cell was completely closed (recombination catalyst inside the cell), the power-in W_{in} can be calculated from EI , where E is the potential in volts and I is the total current in amperes. If the cell allowed the evolved gases to escape, or recombined them outside the cell, the power-in factor must be modified by subtracting the heat of recombination of D₂ and O₂ (the thermoneutral potential), equivalent to 1.54 V/mol⁻¹, from the potential factor.

The most common method of describing the results is in terms of "excess heat," which is given by^b

$$\frac{W_{out} - W_{in}}{W_{in}} \quad (1)$$

^bIn the first year of examining the Fleischmann-Pons effect, there were many papers⁴ that stressed alleged errors in calorimetry. However, for small cells, it is easy to measure (by means of thermistors) the temperature to $\pm 0.01^\circ\text{C}$, and the changes in temperature above those expected are generally $\sim 1^\circ\text{C}$. Particularly if stirring in the cell is good, it would seem difficult to have significant calorimetric errors.

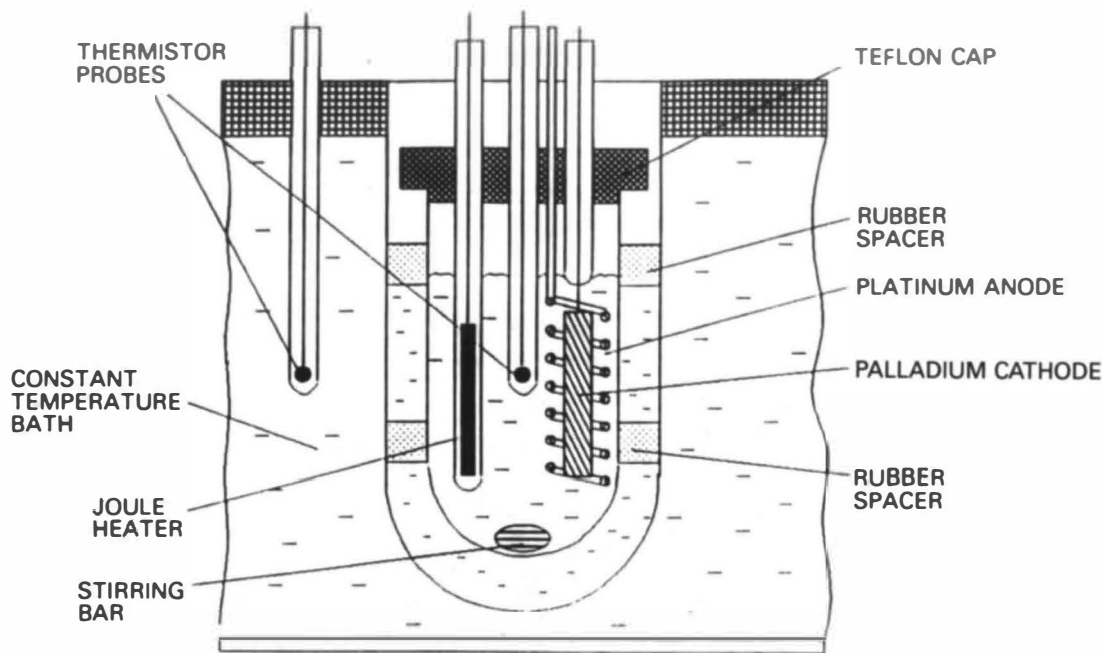


Fig. 1. Schematic of a typical Fleischmann-Pons-type calorimetric cell (not to scale).

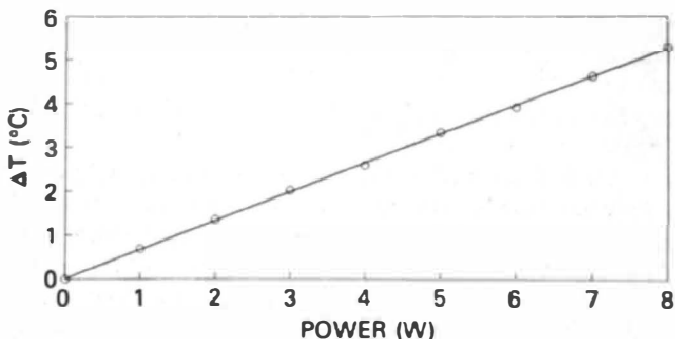
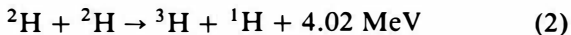


Fig. 2. Typical calibration curve for the cell shown in Fig. 1 (Ref. 3).

This also requires continuous monitoring of potential, current, and ΔT .

MEASUREMENT OF NUCLEAR PRODUCTS

The production of radiation from such cells can be divided into observations of (a) tritium, (b) neutrons, and (c) other types of radiation (including gamma and X rays). The paths leading to the formation of the first two types of radiation are shown below:



and



The production of tritium from reaction (2) is easily characterized by the technique of liquid scintillation counting, in which a scintillating mixture is added to a sample and the resulting excitation analyzed. Several problems, however, exist with this technique. The chemiluminescence of the scintillation cocktail can be mistaken for high tritium activity. Thus, it is imperative that the analyzing instrument be capable of registering the luminescence effect. If any chemiluminescence is detected, the result should be thrown out until the level of chemiluminescence is zero (as will normally occur in a few hours).

A further complication is the buildup of tritium on normal electrochemical grounds. During electrolysis of a solution containing a mixture of the isotopes of hydrogen, a preferential evolution of the lightest isotope occurs – the so-called isotopic separation phenomenon.⁵ Thus, a natural increase in tritium activity is expected. In an alkaline solution, the value of the separation factor is ~2 on palladium (see Table I). As D₂O contains a trace amount of tritium, a natural increase to a value of approximately twice that of the original solution occurs (see Appendix). For example, if the tritium activity is originally 100 disintegrations per minute per millilitre (dpm/ml), after prolonged electrolysis including frequent additions of tritium-containing D₂O, the final value would be expected to be of the order of 200 dpm/ml (on classical grounds).³

If, however, the above sources of error are taken into account, tritium measurement remains the easiest nuclear particle phenomenon to quantify.

Neutron detection is much more complex and far

TABLE I
Values of S_{H-T} and S_{D-T} on Various Metals⁶

Metal	i (mA/cm ²)	S_{H-T}
Palladium	30	6.6
Palladium	100	6.6
Palladium	300	6.9
Platinum	16	7.6
Platinum	32	7.2
Platinum	100	8.8
Titanium	25	6.2
Titanium	75	6.1
Titanium	250	7.0
Iron (pH = 6.5)	20	9.1
Iron (pH = 7.5)	20	9.6
Metal	i (mA/cm ²)	S_{D-T}
Palladium	100	2.6
Palladium	300	1.9
Platinum	20	2.2
Platinum	32	2.6
Platinum	64	2.5
Platinum	80	3.0
Titanium	60	2.2
Titanium	90	2.5
Titanium	90	2.6
Titanium	260	2.6

more expensive. It requires a great deal of equipment and experimental experience. Cosmic-ray showers that lead to false neutron counts require elaborate methods to be detected and rejected. One of the most efficient neutron detectors is the NE-213 liquid scintillator detector. With suitable electronics, this detector has an overall efficiency of ~5%.

The production of other radiative particles (e.g., X rays, gamma rays, etc.) is secondary to the production of neutrons or tritium. Thus, their detection and quantification are not described here. Note, however, that the existence of such particles could provide valuable information regarding the mechanism of any nuclear reaction occurring under such experimental conditions.

ELECTROCHEMICAL EXCESS HEAT PRODUCTION

The production of excess heat can be categorized into two sets of observations: the so-called "low-level" heat, corresponding to an excess heat [as defined in Eq. (1)] <100%, and excess heat >100%. Most reports

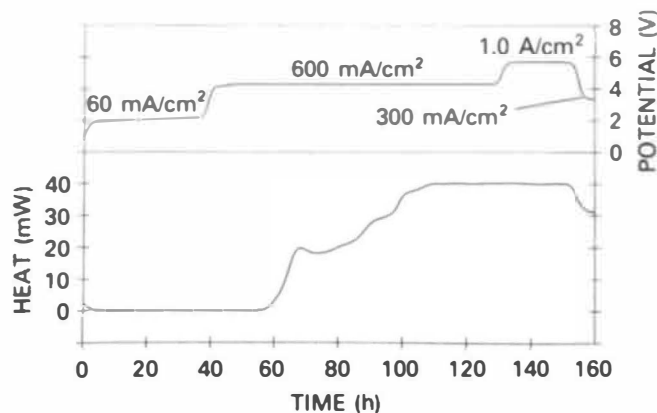


Fig. 3. Appleby and Srinivasan's Pd-D₂O experimental results.⁸

fall into the first category. The excess heat is rarely a constant phenomenon; rather, it occurs in bursts of activity, sometimes, but not always, associated with a change of system parameters (a change in current density, for example). Such heat bursts occur over a broad time span between minutes to days. In only a few cases has it been possible to correlate production of excess heat with production of radiation.⁷

The first reports by Fleischmann and Pons¹ gave a power output of 26 W/cm³, corresponding to an excess heat of ~111%. Their recent claims are of a higher output of ~600%.

Srinivasan and Appleby⁸ at Texas A&M University used an ultrasensitive microcalorimeter in which only very small (0.01-cm³) electrodes can be analyzed. Using this instrument,^c they claim the highest reproducibility rate at ~90% (Fig. 3). The levels of excess heat, however, are only of the order of 10%. Blank cells with H₂O produce negligibly low effects. Replacement of the lithium electrolyte (either ⁶LiOD or ⁷LiOD) by the sodium equivalent (NaOD) reduces excess heat production by ~85% if the replacement is performed when the experiment has been running for some time (Fig. 4). The effect of *starting* with a sodium electrolyte is not yet known.

Kainthla et al.⁹ at Texas A&M have observed excess heat in 4 out of 28 cases (Fig. 5). They used a variety of cells. In some, gases were recombined outside the cell; in others, the cells were closed with a recombination catalyst inside the cell. In general, excess heat of ~10 to 30% was observed, occurring in bursts. In one cell, an excess heat burst was seen with an associated burst of tritium production. Claims of errors in the calorimetry are dealt with by the evidence that when a cell ceases to show excess heat, the heat output falls back exactly on the calibration line. Gas

^cThis calorimeter has stainless steel walls.

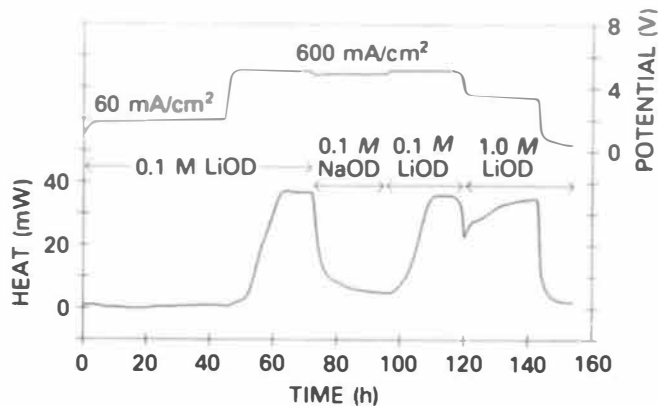


Fig. 4. The replacement of LiOD by NaOD in the Srinivasan and Appleby experiment,⁸ showing almost complete reduction of excess heat.

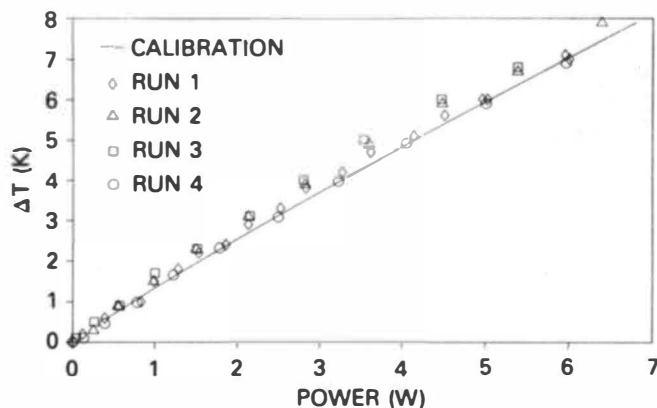


Fig. 5. An example of the excess heat measurement from Kainthla et al.⁹

recombination as another possible error is discounted by the evidence that the faradaic efficiency is 100% ($\pm 2\%$). The absolute power generated in one of these cells corresponds to 9 W/cm^3 .

McKubre¹⁰ at SRI (formerly Stanford Research Institute) (Fig. 6) used a high-pressure D_2 electrochemical cell that reduces anode polarization. This cell was placed in a flow calorimeter that, by means of an electrical heater and electrochemical power, was maintained at a constant total power. Any process that gave heat in excess of this power was detected as an increase in the calorimeter outlet temperature. Results have shown 20 to 50% excess for periods of up to several days. In addition, there is tentative evidence of the production of ionizing radiation from within the palladium cathode.

In addition to calorimetric measurements, researchers at SRI also studied the resistance of the palladium electrode and its interfacial electrochemical impedance. These measurements provide fundamental

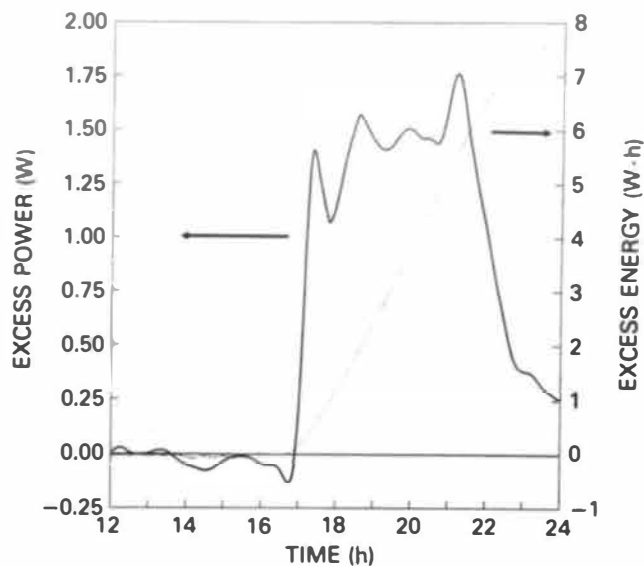


Fig. 6. Excess heat reported by McKubre.¹⁰

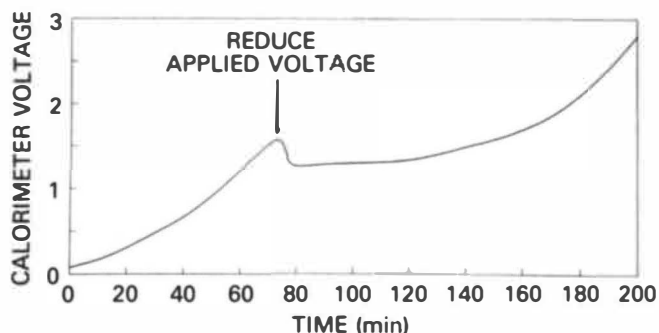


Fig. 7. Excess heat reported by Oriani et al.¹¹

information on the deuterium/palladium (D/Pd) ratio and the nature of the electrochemical kinetic processes occurring at the surface.

Oriani et al.¹¹ at the University of Minnesota observed 100 W/cm^3 in two cells in a heat flow calorimeter. The evolved gases were separated using a glass cylinder between the electrodes, perforated by many small holes to permit ionic conductivity in the cell. These cells were run in a potentiostatic rather than galvanostatic mode. As have many other workers, Oriani et al. observed frequent runs where no excess heat was produced, and the heat output fell exactly on the calibration line. This was also true for several experiments with H_2O . When the cells showed excess heat, they did so in a definite manner, and after a certain waiting period (16 and 22 h of constant input power in this case) (Fig. 7).

Huggins¹² at Stanford University originally observed 7 W/cm^3 of excess heat for 12 days in three out of five cells. This corresponds to 30 to 35% excess.

Recently, he observed 23 to 24 MJ/mol palladium from a closed cell.

Wadsworth et al.¹³ at the University of Utah reported ~ 60 W/cm³ excess in five cells on several occasions. Again, this excess occurred in bursts rather than as a constant phenomenon (Fig. 8).

Champion¹⁴ in Tennessee originally claimed up to 600% excess heat using a radio-frequency (rf) heterodyne beat method. However, the actual amount of rf absorbed into the system was difficult to measure. An on-site visit by researchers at Texas A&M failed to confirm these high levels, but did witness $\sim 60\%$ excess.

Adzic et al.¹⁵ at Case Western Reserve used a cell of the type found in Ref. 1, in a battery-run calorimeter. In two closed cells with palladium in LiOD, a small excess heat was observed over an extended time. With palladium in LiOH or platinum in LiOD, no similar excess was observed. In an open cell, with 4 mm of Johnson-Matthey palladium, a 20 to 45% excess was observed over an extended time. Lithium was found to penetrate 200 nm into the palladium bulk.

Schoessow and Wethington¹⁶ claim up to 400% excess in one cell, and 60% in the other (only two cells have been fabricated).

Santhanam et al.¹⁷ at the Tata Institute reported 0.2 MJ/cm³ after a 48-h period from a titanium cathode using a current density varying from 33 to 66 mA/cm². Corresponding data for a palladium cathode showed no excess heat. Characteristic cracking of the electrode was observed using acoustic emission monitoring equipment.

Hutchinson et al.¹⁸ at Oak Ridge National Laboratory have reported four out of four cells produced 3 W/cm³, equivalent to an 18% excess. Their original claims were for the same levels for one cell out of two after 100 days of charging.

ELECTROCHEMICAL TRITIUM PRODUCTION

In general, the reports of radiation production in Ref. 1 were later discovered to be less certain than at first claimed. However, Schoessow and Wethington¹⁶ and Packham et al.¹⁹ reported the observation of high levels of tritium production in their cells. The normal buildup of tritium from the frequent additions of heavy water (which includes traces of tritium as a contaminant) could not account for the levels of tritium measured in the cells. Packham et al.¹⁹ reported tritium production of 10^2 to 10^4 times the background levels in 14 cells out of 28 (Table II and Fig. 9). Moreover, one particular batch of 1-mm palladium produced tritium in all eight cells. The actual rate of tritium production fell between 10^{10} to 10^{12} atom/s·cm². A thorough search for contamination gave negative results (Tables III and IV). This search included tests of each component of the electrochemical cell, including an analysis of the virgin anode and cath-

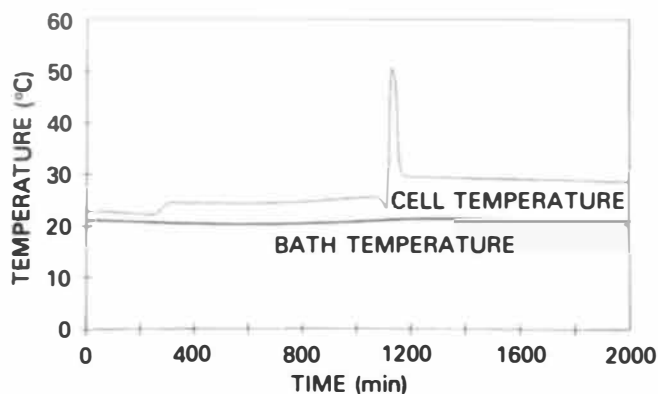


Fig. 8. Excess heat reported by Wadsworth et al.¹³

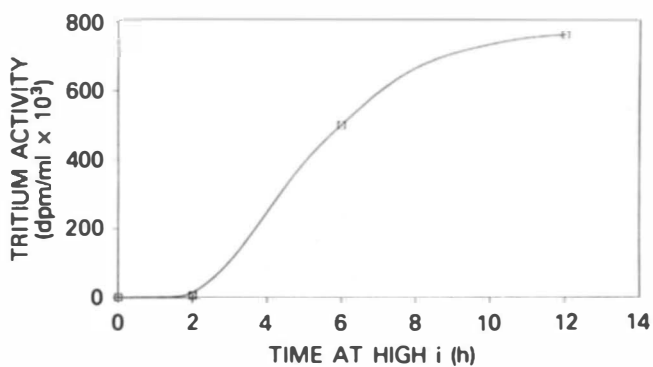


Fig. 9. Tritium production from cell A7 from Packham et al.¹⁹

ode material by Los Alamos National Laboratory²⁰ (LANL). Confirmation of the actual levels of tritium in solution was obtained from three national laboratories and one private institute (Table V). All analyses were performed in a blind fashion.

In one cell, the production of tritium has been correlated with the production of excess heat⁷ (Fig. 10). However, the tritium produced could only account for 0.1% of this excess heat, which was at a level of up to 25%.

Wolf et al.²¹ observed tritium production in one cell at the level of 10^5 dpm/ml (Fig. 11). The tritium in this case was produced in one 12-h burst. After the burst, the tritium was slowly and gradually sparged out, leading to the conclusion that at least part of it was in the form of deuterium-tritium (D-T). Several other cells seemed to show low-level tritium production, above that accountable by separation factor differences alone.

Schoessow and Wethington¹⁶ reported that two cells had produced tritium at levels of 10^5 dpm/ml. They used cathodes in the form of palladium buttons with platinum anodes.

TABLE II
Cell Identification, Electrode Treatment, Solution Type and Tritium Activity of Electrolyte Samples⁶

Cell	Electrode Pretreatment	Solution	Corrected ³ H Activity (dpm/ml)
A1	No treatment	0.1 M LiOD	3.8×10^4
A2	No treatment	0.1 M LiOD + 0.1 mM NaCN	
	After 16 days at 50 mA/cm ² then for 8 h at 500 mA/cm ² (May 1, 1989)		168
	50 mA/cm ² for 4 days (May 5, 1989)		134
	50 mA/cm ² for 3 h, 110 mA/cm ² for 2 h, 200 mA/cm ² for 20 min (May 6, 1989)		1.1×10^4
	50 mA/cm ² (May 7, 1989)		1.4×10^4
	(May 7-13, 1989)		1.1×10^4
	(May 13-June 6, 1989)		7.5×10^3
A3	Anneal	0.1 M LiOD	4.9×10^6
A4	Anneal	0.1 M LiOD + 0.1 mM NaCN	1.2×10^5
A5	Acid etch	0.1 M LiOD	3.7×10^6
A6	Acid etch	0.1 M LiOD + 0.1 mM NaCN	3.3×10^4
A7	Electrochemical	0.1 M LiOD	
	Before high current density		102
	After 2 h at 500 mA/cm ²		5223
	After 6 h at 500 mA/cm ²		5.0×10^5
	After 12 h at 500 mA/cm ²		7.6×10^5
A8	Electrochemical	0.1 M LiOD + 0.1 mM NaCN	
	After 16 days charging and 8 h high current density (May 1, 1989)		192
	Electrolyte levels after 6 weeks at 50 mA/cm ²		5.0×10^5
	Recombined gas levels after 2 weeks of external recombination at 50 mA/cm ²		5.0×10^7
B3 (3 mm)	Anneal	0.1 M LiOD	6.3×10^4
B5 (3 mm)	Acid etch	0.1 M LiOD	48
Cell 1 (6 mm)	No treatment	0.1 M LiOD	117
Cell 4		(See Fig. 10)	
M1	No treatment	0.1 M LiOD	3000

Storms and Talcott²² at LANL fabricated a very large number of cells (>100). They used various poisons of hydrogen evolution in an attempt to drive deuterium into the palladium. To date, 2 cells out of 91 have given high levels of tritium, in addition to 9 cells that have shown levels above the separation factor concentration (Fig. 12). The two cells with high counts had at 9000 and 12000 dpm/ml, respectively. The poisoning approach was also used by Packham et al.,¹⁹ but the addition of 0.1 mM NaCN seemed to lower tritium production in all cases (see Table II). Poisoning with such compounds as CN⁻, thiourea, and other sulfur compounds (Storms and Talcott bubbled H₂S through their solution) is an approach that should be further investigated.

Iyengar et al.²³ at the Bhabha Atomic Research Centre (BARC) have reported the most impressive set of data regarding radiative particles. They report a tritium level of up to 10^5 dpm/ml in six cells. In one case in particular, they used a multicathode array consisting of palladium-silver alloys, in a circular orientation around a central anode. The duration of tritium production varies from as short as 4 h to as long as 49 days. They have investigated the effect of various different electrode materials including the alloys.

Adzic et al.¹⁵ reported the discovery of low levels (up to 40 times background) of tritium in five of their electrochemical cells. The cell with the 40 times increase also showed 20 to 45% excess heat. Three of the fabricated cells had nickel as the anode material.

TABLE III
Blank Experiments During Tritium Analysis¹⁹

Sample	Count/min·ml ⁻¹	Background-Corrected Activity (dpm/ml)
D ₂ O analysis 1	65	48
D ₂ O analysis 2	70	63
D ₂ O analysis 3	67	54
D ₂ O analysis 4	60	33
D ₂ O analysis 5	50	3
D ₂ O analysis 6	71	66
D ₂ O analysis 7	75	78
D ₂ O analysis 8	62	39
0.1 M LiOD analysis 1	75	78
0.1 M LiOD analysis 2	70	63
0.1 M LiOD analysis 3	74	75
0.1 M LiOD analysis 4	65	48
0.1 M LiOD analysis 5	60	33
0.1 M LiOD analysis 6	66	51
0.1 M LiOD analysis 7	76	81
0.1 M LiOD analysis 8	70	63
Neutralized 0.1 M LiOD	73	72
Neutralized 0.1 M LiOD + 0.1 mM NaCN	76	81
Dissolved nickel in acid analysis 1	78	87
Dissolved nickel in acid analysis 2	80	93
Dissolved nickel in acid analysis 3	76	81
Scintillation cocktail	49	---

TABLE IV
Mean of Blank Experiments During Tritium Analysis¹⁹

Sample	Count/min·ml ⁻¹	Background-Corrected Activity (dpm/ml)
BIOSAFE II Cocktail	170 ± 13	---
H ₂ O analysis	161 ± 16	0
D ₂ O analysis	210 ± 16	100
0.1 M LiOD analysis	220 ± 20	125
0.1 M LiOH analysis	157 ± 12	0
Dissolved nickel in nitric acid	140 ± 20	0
Tygon tubing in NaOH	105 ± 20	0
Rubber stoppers in NaOH	150 ± 20	0
Recombination catalyst in NaOH	140 ± 15	0
Dissolved shavings from cutters	160 ± 11	0
Dissolved shavings from vacuum chamber	164 ± 17	0
Dissolved shavings from spotwelder	155 ± 10	0

Malo et al.²⁴ at the Mexican Institute of Petroleum reported levels of 2200 dpm/ml in one cell out of three. Background tritium levels were at 85 dpm/ml. The time course of production resembles other findings in that only separation factor levels were found for up

to 20 h. After 90 h, however, levels had risen to 2200 dpm/ml (Fig. 13).

Guruswamy²⁵ at the University of Utah recently reported finding ~100 times background levels in one cell and low-level production in other cells.

TABLE V
Confirmatory Results from Outside Sources on Various Samples¹⁹

	Sample 1	Sample 2	HTO Standard	0.1 M LiOD	D ₂ O
Texas A&M	2.13×10^6	1157	7.23×10^5	93	47
Battelle	1.96×10^6	1170	8.08×10^5	127	140
Argonne	1.96×10^6	1020	7.59×10^5	90	114
LANL	1.97×10^6	800 to 1300	6.50×10^5	113	161
General Motors	1.80×10^6	1000		Not analyzed	

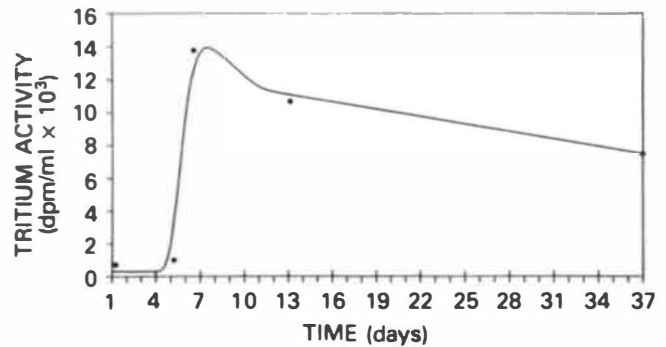
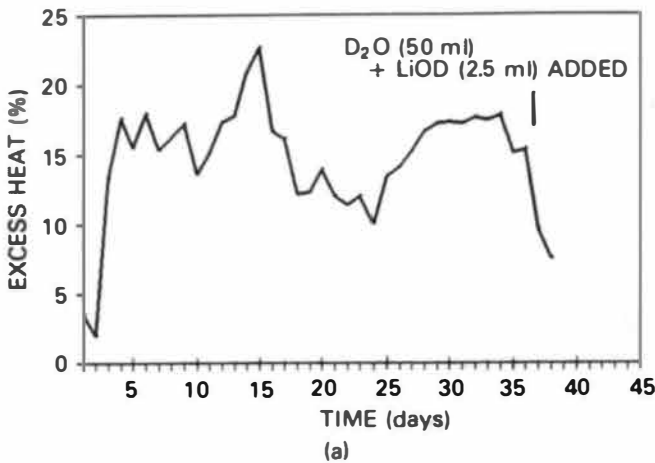


Fig. 11. Tritium production from cell A2 from Wolf et al.²¹

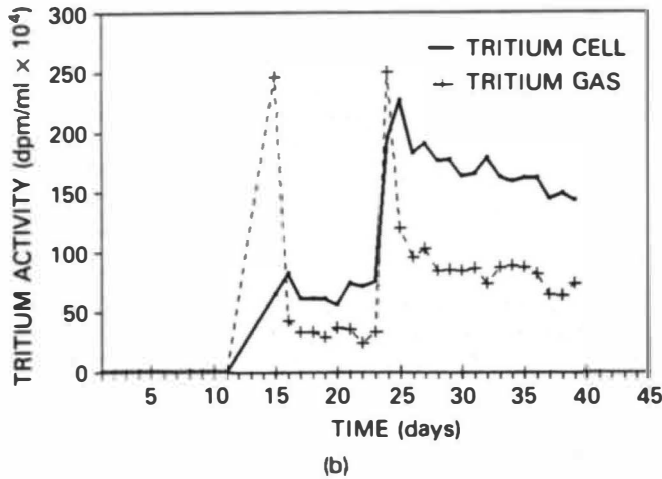


Fig. 10. The concurrent production of (a) excess heat and (b) tritium bursts from cell 4 from Kainthla et al.⁷ The cell was at charging current from July 27, 1989. Time zero here is September 11, 1989.

Scott et al.²⁶ at Oak Ridge National Laboratory reported tritium activity of 25 times the background level in one cell with current densities varying between 200 and 600 mA/cm². This tritium occurred in a burst lasting 2 to 3 h. The typical sparging of tritium from the cell was also observed (Fig. 14).

ELECTROCHEMICAL NEUTRON PRODUCTION

The great difficulty with neutron counting is lowering the background level sufficiently that a small effect can be seen if present. Also, the type of detector used can affect the validity of the results. A method to reject signals from cosmic-ray events must also be included in the experimental apparatus.

Jones et al.² at Brigham Young University used a BC505 neutron detector with a background rate of $\sim 10^{-3}$ n/s and an overall efficiency of 1%. The electrolyte used in this case was a complex mixture of inorganic salts in D₂O, at a pH of ~ 3 . Neutron production was observed at rates up to five standard deviations above background in 11 out of 14 cases (Fig. 15). Jones et al. suggest that if the reaction occurs at the surface or if the conditions favoring fusion occur only intermittently (i.e., the time period for production is considerably less than the measuring time of the detection system), then the inferred fusion rate must be ~ 5 orders of magnitude larger than the detected $\sim 10^{-23}$ fusion/(d-d)·s⁻¹.

Wolf et al.²⁷ observed the production of neutrons at 2.45 MeV in several bursts, at levels between three and five times the background levels. Out of 200 experiments performed, only 3 showed statistically significant neutron emission using the same piece of palladium wire using an NE-213 detector system (Fig. 16). Interestingly, it seems as if the nature of the surface was

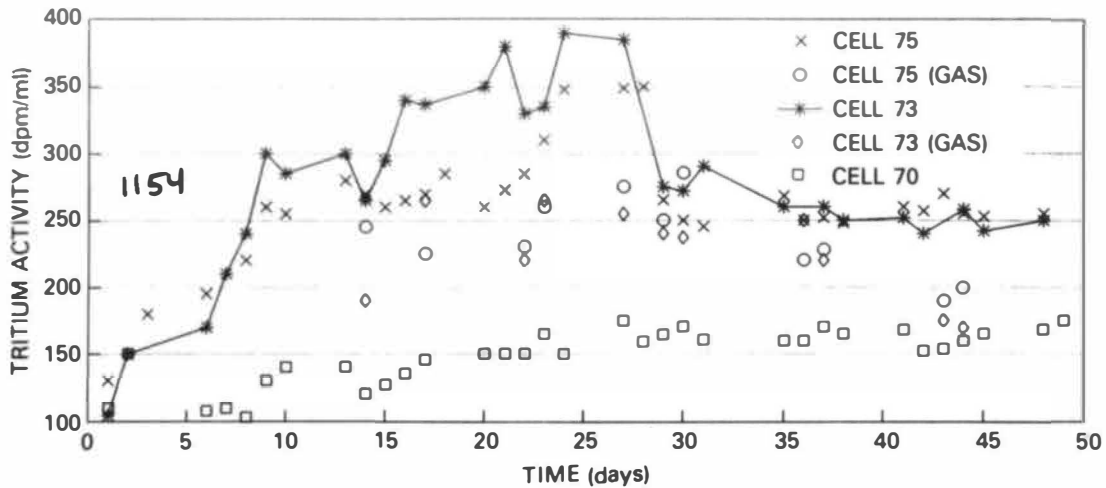


Fig. 12. Tritium production reported by Storms and Talcott.²²

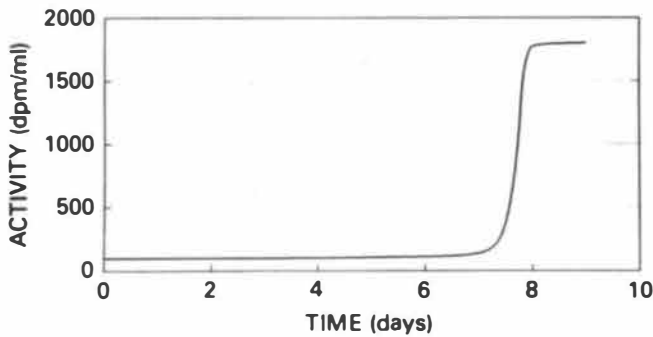


Fig. 13. Tritium production reported by Malo et al.²⁴

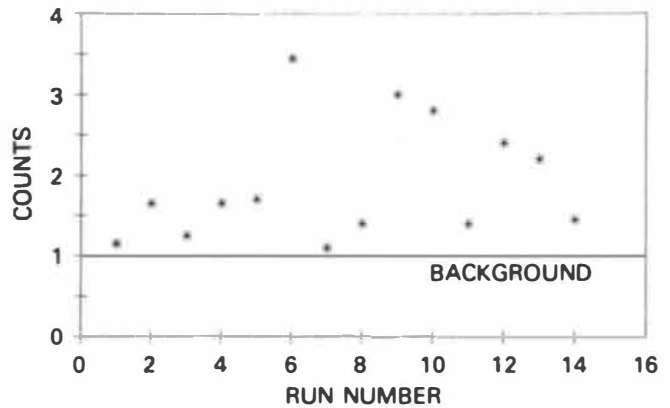


Fig. 15. Neutron production reported by Jones et al.²

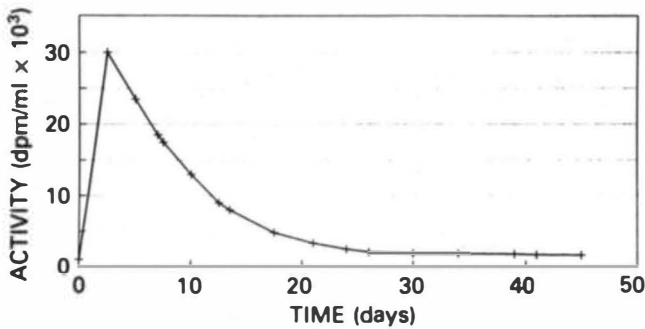


Fig. 14. Tritium production reported by Scott et al.²⁶

directly related to neutron production: When a burst had died down to the background level, the electrode was taken out of solution, physically wiped, and replaced into the solution, and the effect reappeared.

The neutron production rate was ~ 1 n/s and was up to nine standard deviations above the background

signal. The major achievement here was the lowering of the background count rate to <1 n/min. This allowed very low production rates to be measured. In addition, various tests showed that the signal was indeed coming from the cell, and not from a change in the background count rate (Fig. 17). Wolf et al.'s neutron detection system was calibrated using a Pu-Be source, a ²⁵²Cf source, and a ²⁵²Cf time-of-flight (TOF) measurement. This allowed a confidence in interpretation of the energy spectra produced in terms of knowing exactly where 2.45-MeV neutrons would appear. Both active and passive cosmic-ray shielding was in place throughout the course of the experiments, and pulse-shape discrimination was performed on the signal. A check was made to see if the detected events coincided with known cosmic-ray activity. This check proved to be negative.

The BARC results on neutrons²³ were obtained using counters of much lower efficiency than those

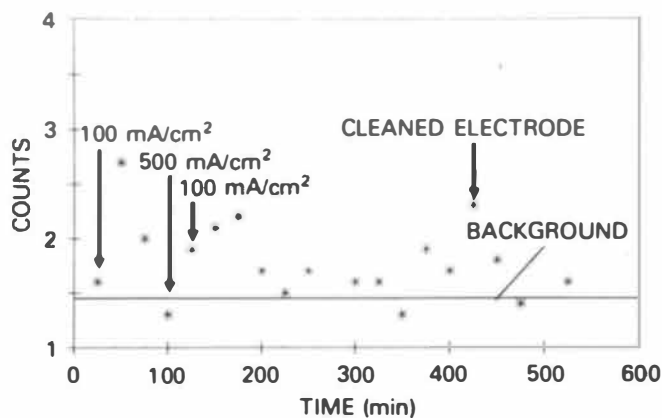


Fig. 16. Neutron production from cell A5 (first occurrence) reported by Wolf et al.²⁷

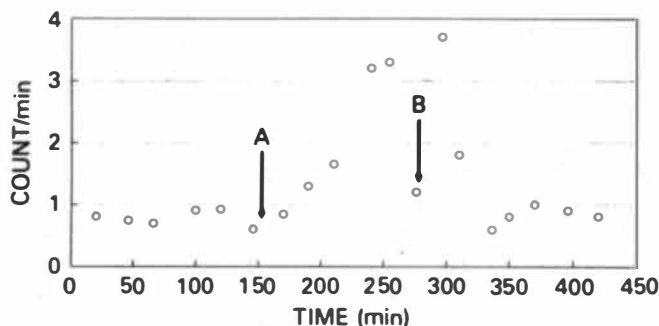


Fig. 17. Neutron production from cell A5 (second occurrence) reported by Wolf et al.²⁷ The cell was inserted in front of the counter at point A and rotated 5 cm away from the counter for the measurement at point B.

at Texas A&M, and with a background count rate of between 2 and 20 n/s (~1000 times higher than Wolf et al.'s experiments). In one of their experiments, a burst of neutron emission occurred for 40 h during an overall electrolysis time of 32 days. The rate of production was maximum at 1.3×10^3 n/s. At least four experiments gave neutron count rates 30 to 1000 times the high background rate (Fig. 18).

The Texas A&M and BARC groups could, therefore, estimate a branching ratio for production. It is significant that both groups measured a branching ratio of between 10^{-8} to 10^{-10} , although one of the BARC experiments did give a branching ratio of 10^{-2} .

OTHER RADIATION FROM ELECTROCHEMICAL EXPERIMENTS

Rolison and O'Grady at the Naval Research Laboratory²⁸ investigated the change in m/z ratios for species in the palladium electrode after electrolysis by time-of-flight secondary ion mass spectrometry (TOF-

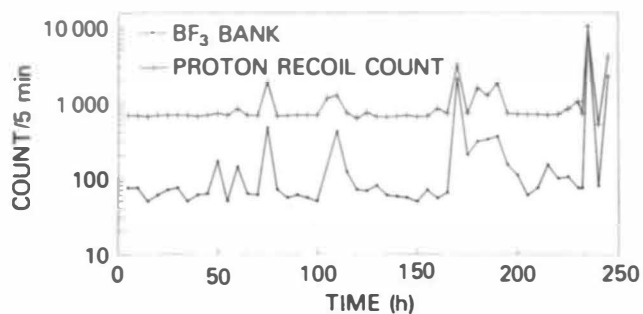


Fig. 18. Neutron production reported by Iyengar et al.²³

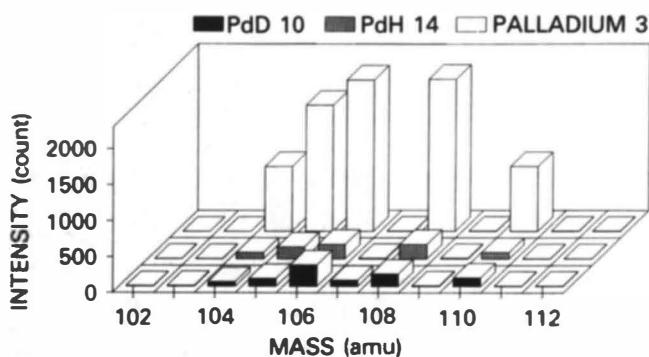


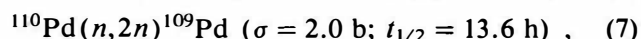
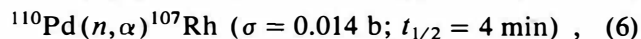
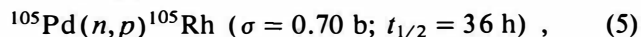
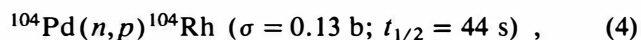
Fig. 19. The m/z ratio changes reported by Rolison and O'Grady.²⁸

SIMS). They found an interesting near-surface enrichment of the m/z 106 species and a near-surface diminution of the m/z 105 and 108 species.

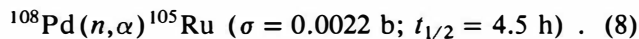
In addition, the low-level impurities ruthenium, silver, and copper were found at significantly higher levels in the near-surface after long-term electrolysis than in the virgin material using X-ray photoelectron spectroscopy.

A blank experiment using palladium electrolyzed in H_2O showed no such enrichment. Mass spectroscopic analyses of the gases evolved when the electrical supply was stopped and showed constituents of m/z 3, 4, 5, and 6 (Fig. 19). The assignments of these values were that they were due to dimers and trimers of the deuterium and hydrogen species, and not due to any tritium-containing species. Therefore, m/z 3 was H_3^+ and DH^+ , m/z 4 was D_2^+ and H_2D^+ , m/z 5 was D_2H^+ , and m/z 6 was D_3^+ . That is, there was no indication of $^3He^+$, T^+ , $^4He^+$, TH^+ , DT^+ , TH_2^+ , T_2^+ , HDT^+ , or Li^+ .

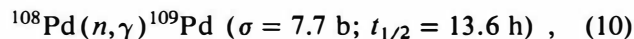
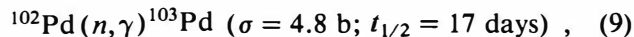
Some of the normal reactions of palladium with 14-MeV neutrons are as follows:



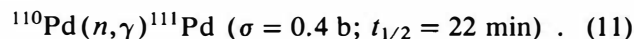
and



In addition, if the fast 14-MeV neutrons were thermalized by the interaction with the aqueous electrolyte, the following reactions could be seen:



and



Although the mass-to-charge data are intriguing, the authors state that it is difficult to explain by any known physical process. However, the spatial orientation of the enrichment suggests a surface mechanism for whatever process is occurring during their electrolysis. It is even more intriguing to note that it is the middleweight species that is enriched at the surface while the heavier and lighter isotopes migrate inward.

The accuracy of the SIMS work presented in Ref. 28 has been questioned, and it is currently being repeated.

An experiment by Taniguchi et al.²⁹ at the Osaka Prefectural Radiation Research Institute reported the detection of charged particles (3-MeV protons). The experiment was designed so that such particles could be measured, since they have a very short mean-free-path. One face of a palladium foil was used, the other side of the electrode being coupled to the radiation detector. There were a total of 30 electrolytic runs. In six of these, significantly higher count rates were observed. Again, the phenomena occurred in bursts. For 6 days, background levels were recorded. On the seventh day, the count rate began to increase and maximized at five times above background (Fig. 20). The time delays in similar runs were 1 day and several hours.

The energy spectra from these experiments show a high count rate of particles with a significantly lower energy than the expected 3.03 MeV [the Q value for the protons emitted in reaction (2)] (Fig. 21). This was ex-

plained by loss of proton energy due to the angle between the path of the particles and the detector. However, it would have been a simple matter to have calibrated the energy spectrum using a 3.03-MeV proton source to see the energy distribution in the detector. Taniguchi et al. have not ruled out other reactions contributing to the phenomena.

GAS-PHASE EXPERIMENTS

In addition to electrochemically loaded palladium and titanium samples, it is possible to load deuterium into such metals by the use of gas pressure. Such loaded materials have also been investigated for radiation production.

Such an experiment was performed by Wada and Nishizawa,³⁰ who passed an ac (60-Hz) 12-kV supply between two palladium electrodes in copper electrode stems in an atmosphere of D_2 gas, in a 1-Pa vacuum.

Neutrons were counted using a BF_3 detector, which had been calibrated with $^{241}\text{Am-Be}$ and ^{252}Cf sources. Two bursts of neutrons were seen after stimulation with the high-voltage source (Fig. 22a). Both bursts corresponded to 14 n/s (up to 2×10^4 times higher than background levels). Interestingly, the pressure of D_2 in the reaction vessel dropped during absorption of D_2 during the charging phase and increased after the first stimulating voltage (corresponding to D_2 being evolved from the palladium), but remained constant after the second stimulating voltage (Fig. 22b). This leads to the conclusion that the deuterium left in the palladium after the first stimulation is held more strongly than the situation before the first stimulation. After the experiment, the residual gases in the chamber were analyzed by mass spectrometry. Substantial amounts of species with mass numbers 1 through 6 were observed.

The results are explained by Wada and Nishizawa as being due to a supersaturated state of deuterium within the palladium. When the rod discards the excess

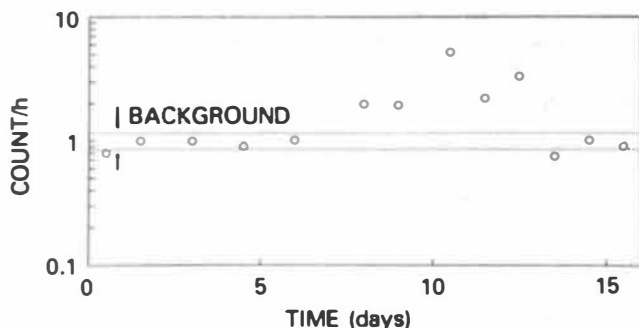


Fig. 20. The production of 3-MeV protons reported by Taniguchi et al.²⁹

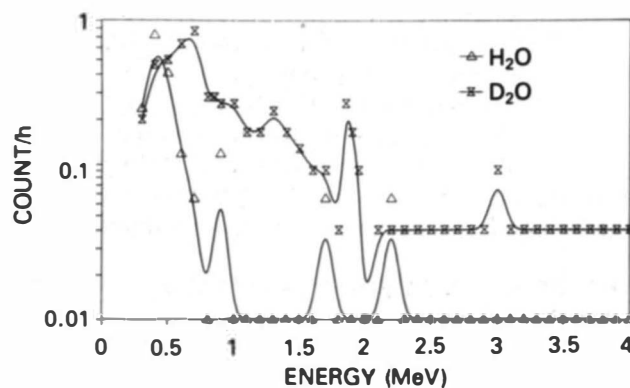


Fig. 21. The energy distribution of 3-MeV protons from Taniguchi et al.²⁹

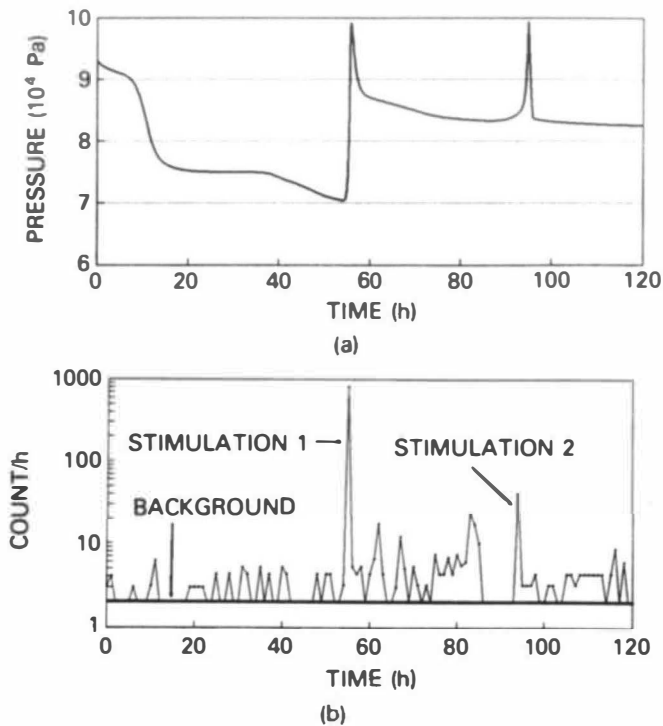


Fig. 22. (a) The gas-phase production of neutrons reported by Wada and Nishizawa³⁰ and (b) the pressure profile of deuterium in the apparatus as a function of time.

deuterium (after the first stimulation), neutrons are emitted. However, no explanation of the mechanism for such neutron production is given.

The experiments run by Menlove et al.³¹ at LANL were performed using both titanium and palladium rods, and the reports contain information on both gas and electrochemically loaded electrodes. Neutrons were detected using ³He detectors. Two different types of neutron phenomena were observed in the gas-phase experiments: one very short ($\leq 100\text{-}\mu\text{s}$) duration, giving 10 to 100 neutrons (Fig. 23), and random neutron counting. The count rates from this experiment were on the order of 0.1 n/s, similar to the Jones et al.² results. Energy analysis of the neutrons was not possible since the yields were too low.

In the electrolytic experiments, two results showed $\sim 3\sigma$ above background, but no definitive statement was made. A third cell gave neutron bursts that continued for several days and was compared to six dummy cells (D_2O cells without electrodes). The largest burst corresponded to a neutron source of 130 neutrons.

Researchers at BARC have also investigated the phenomena in a solid-gas experiment.²³ They used titanium and palladium-silver disks, wafers, and cones, and powdered palladium black. Tritium was found using scintillation counting and autoradiography as well

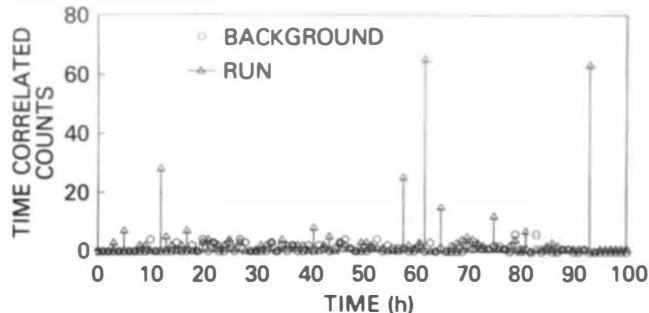


Fig. 23. The gas-phase production of neutrons reported by Menlove et al.³¹

as an X-ray technique. Levels of $>10^{10}$ to 10^{12} atoms of tritium were found.

CLUSTER IMPACT FUSION

An experiment by Beuhler et al.³² at Brookhaven National Laboratory describes a fusion reaction produced by the impact of a cluster of D_2O molecules upon a TiD target. The protons produced from reaction (2) were detected. The accelerating energy of the cluster was varied. At 300-keV, the fusion rate was measured at ~ 0.05 fusion/s. Blank experiments run with an accelerated H_2O cluster on TiD, or a D_2O cluster impacting on a target of TiH, showed no such behavior. The size of the cluster also seemed to be a criterion for fusion reactions occurring. Below a 20 D_2O molecule cluster, no fusion was observed. The peak maximized at ~ 150 molecules and had a broad shoulder up to 1000 molecules (Fig. 24).

THE EXPLOSION PHENOMENON

It seems natural to imagine that explosions might occur in electrolytic cells that are producing a 2:1 mixture of D_2 and O_2 . However, in many circumstances,

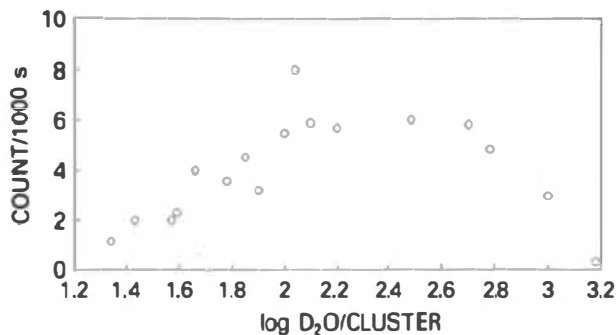


Fig. 24. The dependence of cluster size on neutron production during cluster impact reported by Beuhler et al.³²

it does not seem possible that there is any initiating stimulus in the cell at the time of the explosion. For example, the electrodes are both normally covered by the electrolyte, and it seems unlikely that a spark generated in the solution between the two electrodes could ignite the dissolved gases. In general, the electrode materials are untouched by the explosion, and the glass cell (either the internal or external cell) is ruptured. In several instances, an electrode replaced in the cell after an explosion immediately explodes once again.⁶ In other cases, cells that have been purposely switched off generate sufficient heat so that they are impossible to handle even 1 h later. This phenomenon seems to differ from the ignition phenomenon described in Ref. 1, but cannot be readily explained by a simple D_2/O_2 explosion.

THEORETICAL CONSIDERATIONS

Since Fleischmann and Pons¹ and Jones et al.² reported the cold fusion phenomena, which is difficult to explain by conventional nuclear physics, several attempts to interpret the excess heat as well as radiative particle emission have been made. Such explanations fall into two broad categories: a chemical reaction or nuclear fusion. The heat released by a chemical reaction corresponds to the range of a few electron volts per atom in contrast to the energy liberated in a nuclear reaction—on the order of millions of electron volts per nucleus. In an earlier paper,³³ eight possible chemical contributions to the excess heat seen in Ref. 1 were summarized. It was concluded that any chemical explanation would be improbable (see Table VI). No one chemical explanation suffices to explain the magnitude of the excess heat observed, and the large amount of tritium produced in the solution and gas phase^{6,19} cannot be explained by *any* kind of chemical reaction. The

TABLE VI

Summary of Chemical Contributions to the Fleischmann-Pons Effect

Chemical Explanation	W/cm
Partial exposure of electrode	0.20
Gas-phase recombination	0.30
Surface recombination	0.30
Alpha-beta phase transition	0.03
D/Pd ratio: chemical storage	0.30
Pd- D_2 dissociation: Pauling	0.90
Pd-Li alloy formation	0.08
Total	2.11 ^a

^aCompared to the 26 W/cm³ reported by Fleischmann and Pons.¹ Excess heat in some cases is equivalent to more than 100 times the total heat of sublimation.

second possible explanation is nuclear fusion. Different models to explain the cold fusion experiments have been suggested since they cannot be simply interpreted by existing nuclear physics.

There are two main characteristics of the cold fusion experiments. One is the large tritium-to-neutron ratio, on the order of 10^8 , and the other is the burst-like nature and irreproducibility of the phenomena. A suitable cold fusion theory or model *must* explain both of these two features. The fusion models put forward can be divided into two parts. One is a hot fusion mechanism, which may be either caused by the development or collapse of cracks within the metal lattice, or triggered by cosmic rays. The second is a cold fusion mechanism that may also be divided into two sections: bulk and surface models.

Hot Plasma Explanation

Several workers have suggested that nuclear fusion occurs within some special areas of the palladium or titanium metal, where a hot plasma is formed. Mayer et al.³⁴ suggested that equal electric charges of opposite sign may be generated on each side of a crack as the crack spreads under the strong internal stresses caused by electrolysis (Fig. 25). As the crack grows, the charged surfaces separate while maintaining the constant electric charge, therefore increasing the voltage drop across the crack. A deuteron in the crack may be accelerated, under this large electric voltage drop, to an energy sufficient to overcome the mutual nuclear coulomb barrier. Gajda et al.³⁵ proposed that high-density and temperature pocket plasmas may be formed when defects or cracks in the metal electrode collapse. Hot nuclear fusion may occur in such plasma zones (Fig. 26). Seitz³⁶ suggested that the enthalpy of the formation of a D_2 molecule from the deuteron

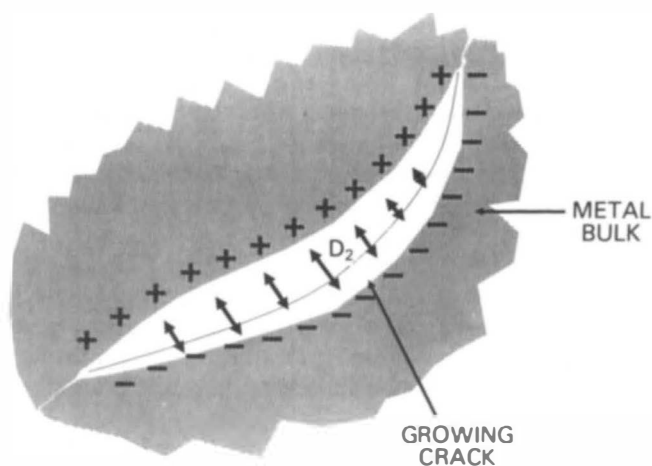


Fig. 25. The growing crack model proposed by Mayer et al.³⁴

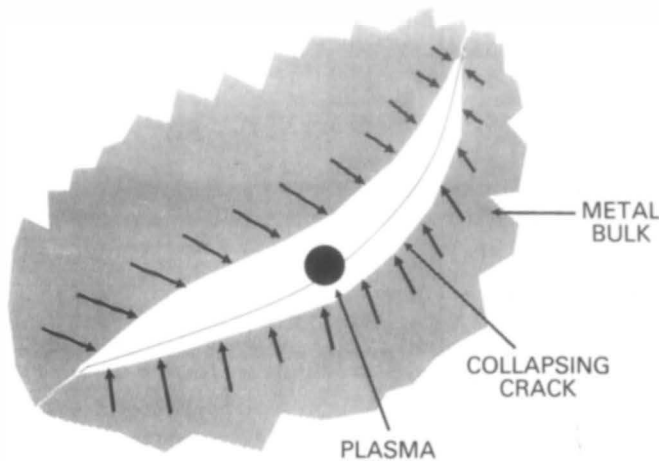


Fig. 26. The collapsing crack model proposed by Gajda et al.³⁵

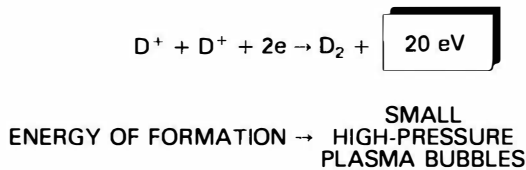


Fig. 27. The formation of plasma bubbles proposed by Seitz.³⁶

within the solid state, which is ~20 eV, will produce small, hot, high-pressure plasma bubbles (Fig. 27). Nuclear fusion would occur in these locally very hot plasma zones. However, as Seitz points out, the surrounding cool metal would quickly quench the hot plasma.

Muon-Catalyzed Fusion

Muon-catalyzed nuclear fusion, triggered by cosmic rays, is another possible origin of cold fusion phenomena (Fig. 28). If a muon is trapped by a deuteron, the internuclear distance of the two deuterium nuclei would be reduced by a factor of ~200, relative to the spacing of normal deuterium nuclei. The muomolecular ion then has a very large cross section for nuclear fusion, a secondary muon being produced. Thus, one muon may catalyze a large number of fusion events, e.g., 200, before it is eventually absorbed by a metal atom. However, in palladium metal loaded with deuterium, placed in a muon beam, negative results were obtained,³⁷ which may indicate that the absorption of muons by the palladium lattice is too large to catalyze nuclear fusion.

Both hot plasma and muon-catalyzed fusion are grouped events. However, Shyam et al.³⁸ claim that such grouped events would appear with a probability of <20%, based on the statistical measurement of neu-

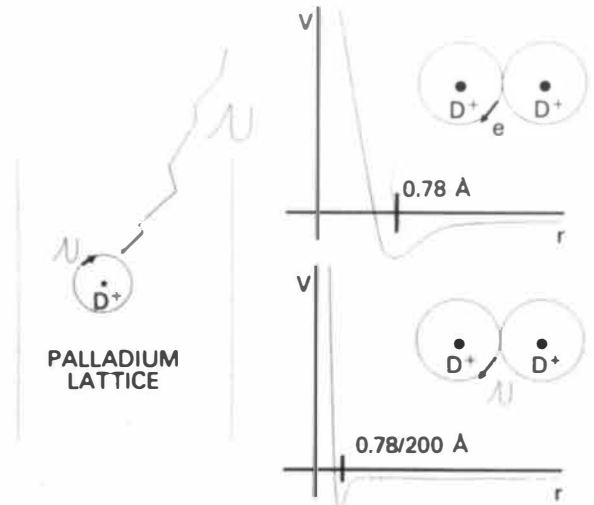


Fig. 28. The muon-catalyzed model proposed by Jones et al.²

tron production in cold fusion experiments. In addition, neither of these two models can account for the observed anomalous branching ratio.

Cold Fusion in Condensed Matter

A different theory is that the deuteron fusion rate is greatly enhanced in the condensed matter environment because of the combination of mutual Coulomb potential screening, the effective mass change, and resonance phenomena (Fig. 29).

In palladium or titanium metal, the coulomb barrier between two deuterons is greatly suppressed by the mobile electrons in the solid-state environment. Crowley³⁹ surmised that the absorbed deuterium in the metal was compressed to a high density to form a dense plasma of liquid metallic deuterium and hence developed a strongly coupled plasma model to account for the electron screen. Leggett and Baym^{40,41} considered a many-body screening effect in the solid-state environment and discovered an unusual enhancement of the nuclear fusion rate. However, the calculated fusion rates were still too low to explain the experimental observations. Horowitz⁴² and Burrows⁴³ modeled the metallic deuteride as a degenerate fermi gas of electrons and calculated the screening Coulomb potential. The calculated effective Gamov penetration factor was increased substantially in the metal environment. They claimed that the (p-d) reaction rate would be larger than or comparable to the (d-d) fusion rate in their model, and the distance between two deuterons would have to reduce to <0.1 Å in order to match the experimental results. However, *ab initio* calculations based on density function⁴⁴ and a pseudopotential total energy approach⁴⁵ showed that the distance between two deuterons in the palladium structure is on the

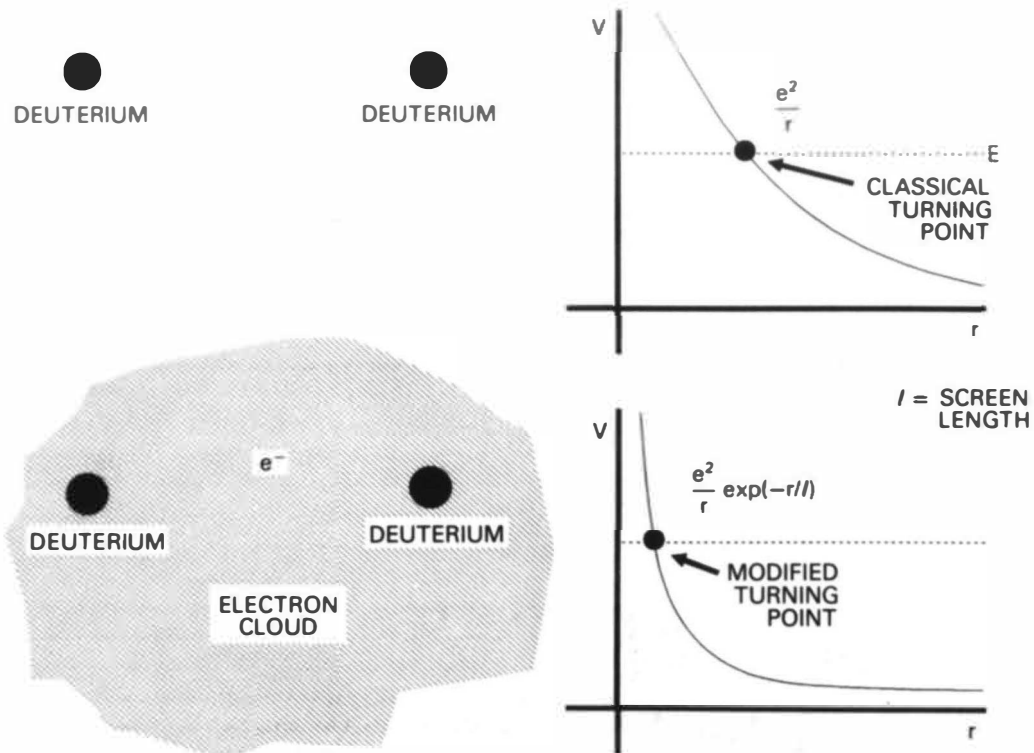


Fig. 29. The effect of electron screening in the palladium lattice.

order of 1 Å. Benesh and Vary⁴⁶ considered that the deuterons in the metal were confined to the bottom of a potential well with electrostatic screening of electrons present in the metal and hence calculated the penetration factor. The results showed that the calculated fusion rate was not sufficient to match the experimental value.

Vaidya and Mayya⁴⁷ modeled the deuterons as a mobile species in the palladium under electrolytic conditions (Fig. 30). A combined screen of Coulomb potential by itinerant deuterons and conduction electrons was considered. Ghosh et al.⁴⁸ proposed that delocalized deuterons in a uniform negative charge distribution of electrons formed a quantum plasma of bosons,

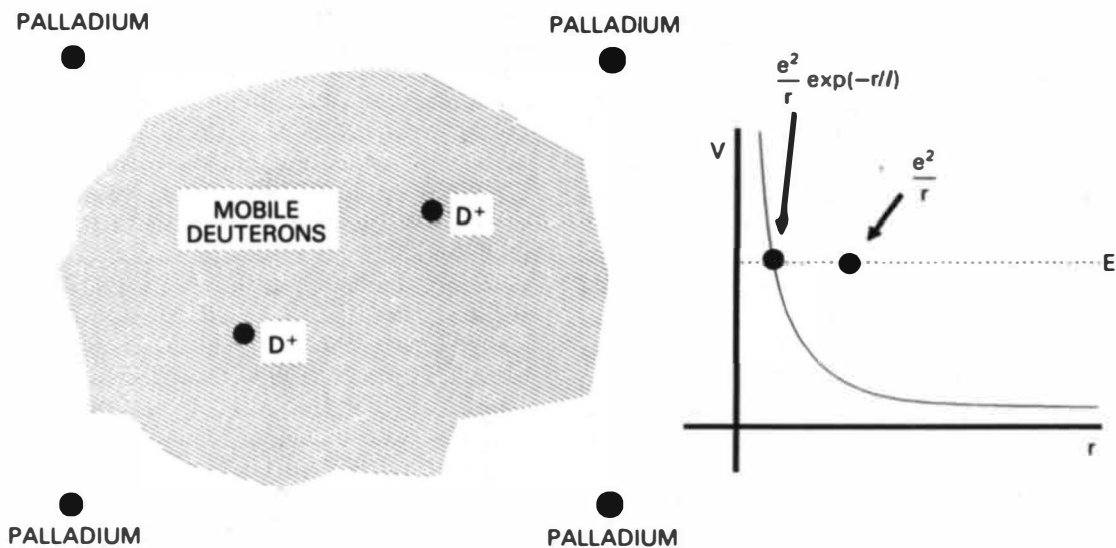


Fig. 30. The effect of mobile deuterons in the palladium lattice.

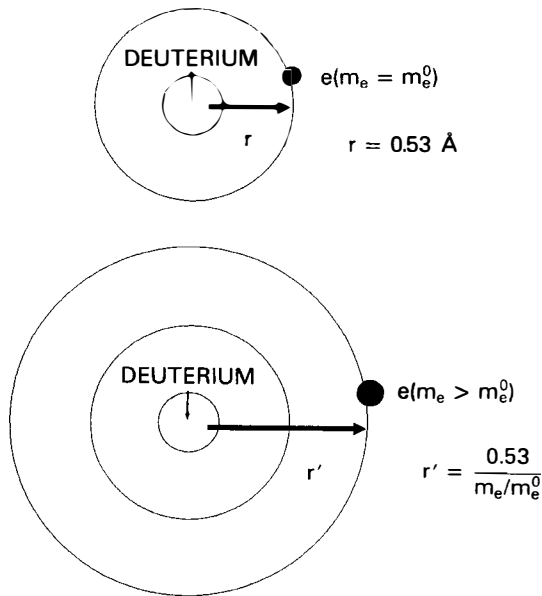


Fig. 31. Electron effective mass increase.

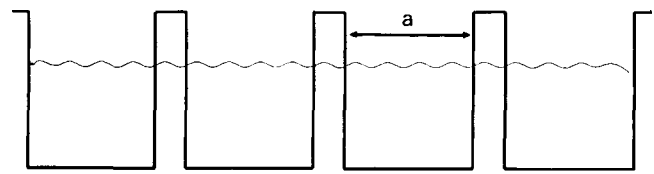
and such collective phenomena leads to a drastic enhancement of the nuclear fusion rate. The fusion rates calculated by Vaidya and Ghosh compare well with experimental values. However, the assumption that all the deuterons in the metal are fully mobile or delocalized may be questionable.

The effective mass change of an electron or deuteron in a heavily deuterated metal compresses the Coulomb potential barrier and enhances the fusion rate (Fig. 31). Jones et al.² proposed that high-effective-mass quasi-electrons formed in the deuterated metal lattice compresses the separation of deuterons and therefore enhances the quantum penetration factor. Tajima et al.⁴⁹ suggested that the deuterium electron and the conducting electrons of the metal form a screening electron cloud with an effective mass greater than the rest mass of the electron. They also calculated the decrease of the Coulomb barrier height by a dielectric medium constructed of core electrons and nuclei of metal atoms. Rabinowitz and Worledge⁵⁰ hypothesized that deuterons in the metal lattice move in a periodic potential well (Fig. 32). These deuterons behave as if they have a reduced effective mass. The tunneling probability of deuterons is then drastically increased. The electron screening of the Coulomb potential barrier was also considered in their model.

A deuteron moving in the metal lattice may find a local potential minimum and be confined in this quasi-stationary structure. Goldanskii and Dalidchik⁵¹ suggested that, under the right conditions, resonance transparency may occur, which would greatly increase the effective collision frequency to a factor of 10⁹ greater than that of the normal frequency, and hence

GAMOW FACTOR

$$G = \exp \left[-\frac{\pi e^2}{\hbar} \left(\frac{M}{E} \right)^{1/2} \right]$$



PERIODIC POTENTIAL

$$m = \frac{\hbar^2}{2a^2 E} - 0.01 M$$

Fig. 32. Deuteron mass decrease.

enhance the nuclear fusion rate by the same ratio (Fig. 33).

However, the enhancement of the Coulomb barrier penetration factor in a metal environment, caused by screening effects of electrons and deuterons, an effective mass change of the electron and deuteron, and the occurrence of a resonance condition, cannot explain the sporadicity and irreproducibility shown in the cold fusion experiments.

Modeling the Quantum Barrier

Turner⁵² hypothesized that transmission resonance on the atomic scale enhanced coulomb barrier tunneling. When the resonance condition

$$\int k(x) dx = \left(n + \frac{1}{2} \right) \pi \tag{12}$$

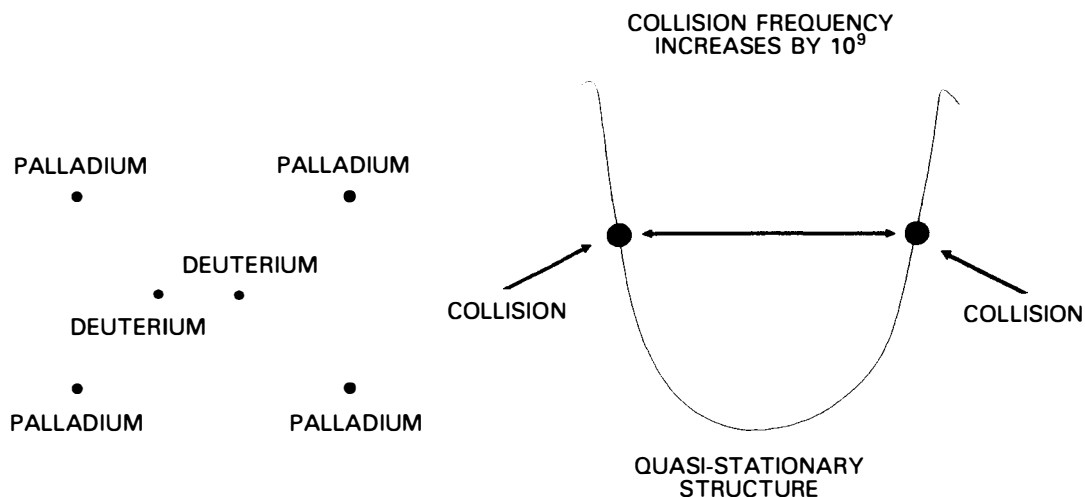
is satisfied by the wave number of the particle crossing the potential well between two barriers, the transmission coefficient is 1. Based on Turner's suggestion, Bush⁵³ proposed a transmission resonance condition:

$$(2n + 1)\lambda/4 = L, \tag{13}$$

with $n = 0, 1, 2, \dots$ for the de Broglie wavelength of the particle within the lattice of a metal deuteride (Fig. 34). He calculated the resonance temperature for deuterons in the palladium deuteride and titanium deuteride lattices. Danos⁵⁴ considered both regular (exponentially decreased) and irregular (exponentially increased) solutions to the calculation of Coulomb barrier penetration. To obtain the ground state of the product nucleus, a third particle, the metal nucleus, was required. A substantial enhancement of the fusion rate was obtained.

Neutron Capture by Palladium

Jackson⁵⁵ suggested a chain reaction mechanism involving the radiative capture of neutrons by palladium nuclei (Fig. 35). A neutron is captured by a palladium nucleus to produce a different isotope of



$$\text{FUSION RATE} = \left(\text{TUNNELING PROBABILITY} \right) \left(\text{COLLISION FREQUENCY} \right) \left(\text{FUSION PROBABILITY} \right)$$

Fig. 33. The quasi-stationary state model proposed by Goldanskii and Dalidchik.⁵¹

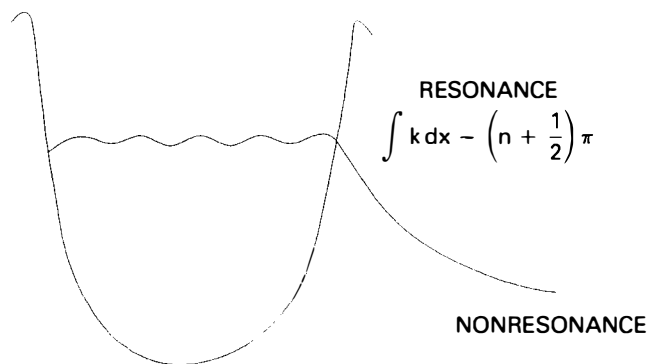


Fig. 34. Resonance tunneling as proposed by Bush.⁵³

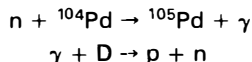


Fig. 35. The chain reaction model involving gamma-ray propagation.

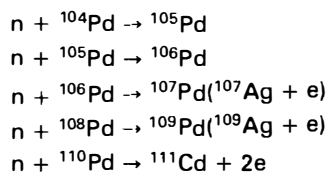


Fig. 36. The radiative capture model proposed by Budelov.⁵⁶

palladium and a gamma photon, which causes photo-disintegration of the deuteron and liberates another neutron. The chain reaction would be propagated in this way. The initiation of the chain reaction may be the enhanced deuteron density within the palladium lattice. Budelov⁵⁶ suggested that nuclear fusion released a neutron within the palladium lattice that would be absorbed by different natural isotopes of palladium (Fig. 36). The by-products would be heat and electrons. Rolison and O'Grady²⁸ observed the near-surface enrichment of ¹⁰⁶Pd and the near-surface diminution of ¹⁰⁵Pd and ¹⁰⁸Pd after electrochemical loading with deuterium in a palladium electrode. Jackson and Budelov's theory may explain the low neutron production rate compared to the high excess heat output. It would seem that radiative capture of neutrons by the metal nuclei may play a part in the cold fusion phenomena.

Quantum Electrodynamic

Jandel⁵⁷ suggested that nuclear fusion occurs in a hypothetical, strongly coupled, confining phase of the quantum electrodynamic domain (CQED), where an electric charge is confined, in analogy to color confinement in quantum chromodynamics. Electrons in the metastable CQED regime are always bound to either a positron forming an electromeson or an atomic nucleus forming an electronucleus. Deuterons may diffuse into the CQED regime, where fusion occurs with a very high rate, possibly attaining the order of 10¹¹ fusion/s. The released fusion energy would then be used to expand and stabilize the CQED domain, which would grow spontaneously in a deuterium-rich environment (Fig. 37). The main product of such a nuclear

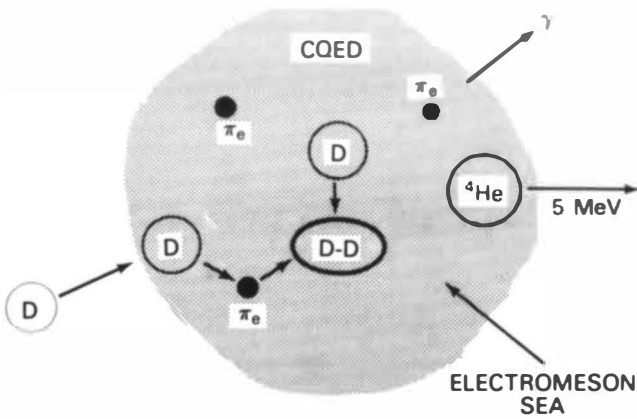


Fig. 37. The CQED model.⁵⁷

reaction would be ${}^4\text{He}$, which would diffuse out of the CQED domain, with a kinetic energy of ~ 5 MeV. The initiation of CQED domains may come from the large transient electromagnetic fields created, for example, by spontaneous fission of unstable transuranic nucleus, which exist in the palladium electrode as impurities. This model can explain the low neutron production compared to the excess heat, as well as the sporadicity of the experiment. However, this model predicts that the tritium output would be less than the neutron production, which is not consistent with experimental observations.

Superradiance

Bressani et al.⁵⁸ have discussed the cold fusion phenomenon based on a superradiant coherent interaction between matter and the electromagnetic field. The released fusion energy would be rapidly cooled by the quantized electromagnetic wave, which would explain the larger amount of excess heat compared to nuclear products.

Surface Model

All the models described above assume that fusion occurs *within* the electrode. However, the experimental observations seem to suggest that the *surface* of the electrode might be the site of such reactions. Specifically, it is suggested⁶ that fusion reactions occur at specific points, or protuberances, on the surface of the electrode. Rolison and O'Grady's experimental observations of palladium isotope ratio shifts²⁸ suggest that the reaction is indeed surface, or near-surface, in nature. Jiang et al.⁵⁹ showed that the fusion reactions occurred only on minute areas of the electrode surface. Lin et al.^{6,60} suggested a surface model, where dendrites grow during prolonged electrolysis on the electrode surface. The main components of the dendrites are impurities, such as nickel and copper, as well as the platinum anode material. Such a hypothesis is consistent with the sporadicity observed in the experiments.

It is well known that a very high electric field exists at the tip of a growing dendrite during electrolysis. When a deuterium gas layer grows on the tip of such

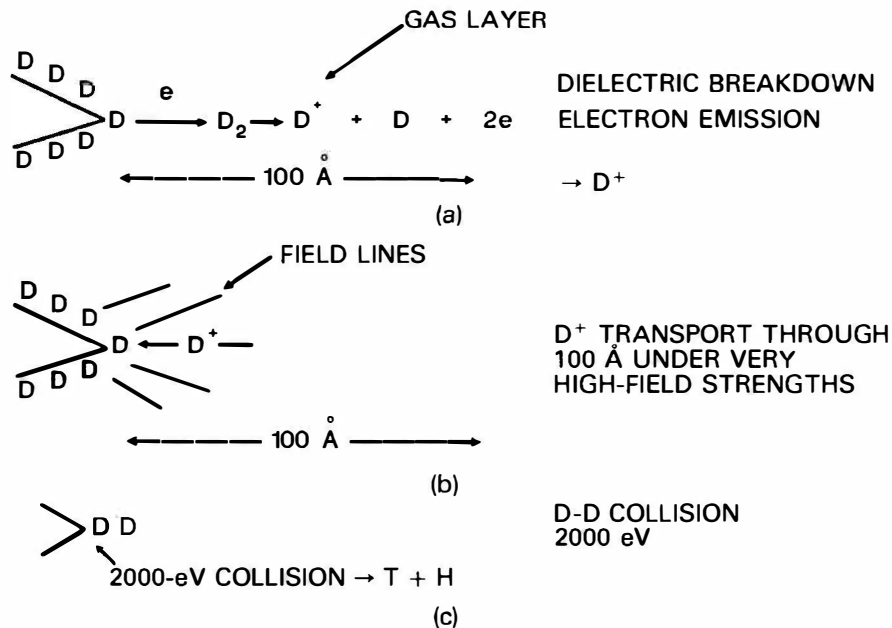


Fig. 38. The dendrite enhanced tunneling model proposed by Lin et al.,⁶⁰ accounting for all the observed phenomena.

a dendrite, an electron, emitted from the tip of the dendrite under the influence of the extremely high electric field, ionizes the deuterium to form a deuteron ion, which is accelerated to a high energy toward the electrode. The high-energy deuteron then collides with another deuteron adsorbed on the tip of dendrite, the resulting collision overcoming the Coulomb potential barrier for quantum tunneling (Fig. 38). Calculated fusion rates compare quantitatively with the experimental results. It is also suggested that the neutron-tunneling transfer reaction $d + d \rightarrow t + p$, similar to the Philips-Oppenheimer stripping phenomenon,⁶¹ may occur with a greater probability, compared to the proton tunneling transfer reaction, in the dendrite surface condition. This model can effectively explain both the sporadicity and irreproducibility of the cold fusion experiments because of the characteristics of the growing dendrite, and also the large tritium-to-neutron ratio.

To summarize, a large number of models have been suggested to explain the experimental observations of the Fleischmann-Pons phenomena. The main characteristics of such phenomena are the large branching ratios of tritium-to-neutrons, $\sim 10^8$, and the sporadicity of the fusion experiments. Of the models discussed, only two, the QCED model suggested by Jandel⁵⁷ and the surface model proposed by Lin et al.,⁶⁰ can account for the sporadicity of the effect. However, as mentioned above, the CQED model would predict a *reverse* tritium/neutron ratio, which contradicts the experimental results.

Hence, at present, the only model that can completely explain the experimental observations or sporadicity and irreproducibility is that proposed by Lin et al.⁶⁰

APPENDIX

Two experimental arrangements have been used here. One involves a cell from which deuterium and oxygen were allowed to escape freely into the atmosphere. Fresh D_2O containing 200 dpm/ml of tritium was added at intervals of 12 to 24 h. The buildup of tritium in solution, with no fusion, can be obtained as follows.

Changes in the tritium concentration occur due to the addition of fresh D_2O containing tritium and removal by electrolysis. The rate of addition of fresh D_2O into the cell R , in order to keep the volume V constant, must be equal to the rate of electrolysis of D_2O ; i.e., $R = i/2F$. Thus, the rate of electrolysis of tritium out of the cell must be equal to the amount replenished by fresh solution and is given by this rate ($i/2F$) times the mole fraction of tritium in solution, or $[Rn_T(0)/n]$, where $n_T(0)/n$ is the mole fraction of tritium and n is the concentration of all hydrogen, deuterium, and tritium species in the solution. The rate of removal of tritium through electrolysis is equal to R_T .

Thus, the factors affecting the concentration of tritium in the electrolyte can be related by

$$Vdn_T(t)/dt = Rn_T(0)/n - R_T \quad (\text{A.1})$$

Let S be the isotopic separation factor of tritium to deuterium, defined as

$$S = (n_D/n_T)_g / (n_D/n_T)_s \quad (\text{A.2})$$

Equation (A.2) can be rewritten as

$$S = (R_D/R_T) / [n_D/n_T(t)] \quad (\text{A.3})$$

where

R_D = rate of production of deuterium atoms

n_D = concentration of deuterium in the solution.

Under experimental conditions, $R_D \sim R$ and $n_D \sim n$; then we have

$$R_T = Rn_T(t)/nS \quad (\text{A.4})$$

Substitution of Eq. (A.4) into Eq. (A.1) and integration gives

$$n_T(t)/n_T(0) = S - (S - 1)\exp(-t/\tau) \quad (\text{A.5})$$

with the tritium buildup time constant τ equal to

$$\tau = SnV/R \quad (\text{A.6})$$

Equation (A.5) shows that the maximum tritium concentration in the solution due to isotopic separation at infinitely long times is S times the tritium concentration in the original solution.

According to Ref. 5, $S = 1.7$ to 2.2 and is hence taken to be 2 . Thus, the time constants for a charging cell with a 15-ml volume and a total current of 0.15 A and for a calorimetric cell with a 100-ml volume and total current of 0.5 A are 22.2 and 44.4 days, respectively.

In the other situation, deuterium and oxygen are recombined outside the cell and the resulting D_2O is reintroduced into the cell. In this case, as no tritium is lost due to the electrolysis and no fresh solution is added, Eq. (A.1) becomes

$$Vdn_T(t)/dt = 0 \quad (\text{A.7})$$

giving $n_T(t) = \text{constant} = n_T(0)$, showing that in this case the concentration of tritium should remain constant in the absence of any nuclear reaction.

ACKNOWLEDGMENTS

We are grateful to the many workers in this field who gave their time to discuss recent results and possible theoretical explanations.

Financial support for the work performed at Texas A&M was provided by the Electric Power Research Institute.

REFERENCES

1. M. FLEISCHMANN and S. PONS, "Electrochemically Induced Nuclear Fusion of Deuterium," *J. Electroanal. Chem.*, **261**, 301 (1989).
2. S. E. JONES et al., "Observation of Cold Nuclear Fusion in Condensed Matter," *Nature*, **338**, 737 (1989).
3. G. H. LIN, R. C. KAINTHLA, N. J. C. PACKHAM, O. VELEV, and J. O'M. BOCKRIS, *Int. J. Hydrogen Energy* (to be published).
4. N. S. LEWIS et al., "Searches for Low-Temperature Nuclear Fusion of Deuterium in Palladium," *Nature*, **340**, 525 (1989).
5. S. SRINIVASAN, "Mechanism of Electrolytic Hydrogen Evolution—An Isotope Effect Study," PhD Thesis, University of Pennsylvania (1963).
6. N. J. C. PACKHAM, Z. MINEVSKI, O. VELEV, and J. O'M. BOCKRIS, Texas A&M University, Unpublished Results (1989).
7. R. C. KAINTHLA, O. VELEV, N. J. C. PACKHAM, L. KABA, and J. O'M. BOCKRIS, *Proc. Conf. Cold Fusion Phenomena*, Washington, D.C., October 1989.
8. S. SRINIVASAN and A. J. APPLEBY, *Proc. Conf. Cold Fusion Phenomena*, Washington, D.C., October 1989.
9. R. C. KAINTHLA, O. VELEV, G. H. LIN, N. J. C. PACKHAM, M. SZKLARCZYK, J. C. WASS, and J. O'M. BOCKRIS, "Sporadic Observation of the Fleischmann-Pons Heat Effect," *Electrochim. Acta.*, **34**, 1315 (1989).
10. M. McKUBRE, SRI, Private Communication (Feb. 1990).
11. R. A. ORIANI, J. C. NELSON, S.-K. LEE, and J. H. BROADHURST, "Calorimetric Measurements of Excess Power Output During the Cathodic Charging of Deuterium into Palladium," *Nature* (to be published).
12. R. HUGGINS, Stanford University, Private Communication (Jan. 1990).
13. M. E. WADSWORTH, S. GURUSWAMY, J. G. BYRNE, and J. LI, *Proc. Workshop Cold Fusion Phenomena*, Santa Fe, New Mexico, May 23–25, 1989.
14. R. CHAMPION, Private Communication (Sep. 1989).
15. R. ADZIC, D. GERVASIO, I. BAE, B. CAHAN, and E. YEAGER, Case Western Reserve, Private Communication (Jan. 1990).
16. G. J. SCHOESSOW and J. A. WETHINGTON, University of Florida, Gainesville, Private Communication (May 1989).
17. K. S. V. SANTHANAM, J. RANGARAJAN, O'N. BRAGANZA, S. K. HARAM, N. M. LIMAYE, and K. C. MANDAL, "Electrochemically Initiated Cold Fusion of Deuterium," *Indian J. Technol.*, **27**, 175 (1989).
18. D. P. HUTCHINSON, C. A. BENNETT, R. K. RICHARDS, J. S. BULLOCK IV, and G. L. POWELL, "Initial Calorimetry Experiments in the Physics Division—ORNL," ORNL/TM-11356, Oak Ridge National Laboratory.
19. N. J. C. PACKHAM, K. L. WOLF, J. C. WASS, R. C. KAINTHLA, and J. O'M. BOCKRIS, "Production of Tritium from D₂O Electrolysis at a Palladium Cathode," *J. Electroanal. Chem.*, **270**, 451 (1989).
20. M. M. FOWLER, Los Alamos National Laboratory, Private Communication (Sep. 1989).
21. K. L. WOLF, N. J. C. PACKHAM, D. E. LAWSON, J. SHOEMAKER, F. CHENG, and J. C. WASS, *Proc. Cold Fusion Phenomena*, Santa Fe, New Mexico, May 23–25, 1989.
22. E. STORMS and C. TALCOTT, "Electrolytic Tritium Production," *J. Fusion Technol.* (to be published).
23. P. K. IYENGAR and M. SRINIVASAN, Eds., "BARC Studies in Cold Fusion," BARC-1500, Bhabha Atomic Research Centre (Nov. 1989); see also *Fusion Technol.*, **18**, 32 (1990).
24. J. M. MALO, J. MORALES, B. ZAMORA, F. P. RAMIREZ, and O. NOVARO, Mexican Institute of Petroleum, Private Communication (Aug. 1989).
25. S. GURUSWAMY, University of Utah, Private Communication (Nov. 1989).
26. C. D. SCOTT, J. E. MROCHEK, E. NEWMAN, T. C. SCOTT, G. E. MICHAELS, and M. PETEK, "A Preliminary Investigation of Cold Fusion by Electrolysis of Heavy Water," ORNL/TM-11322, Oak Ridge National Laboratory (Nov. 1989).
27. K. L. WOLF, D. E. LAWSON, J. C. WASS, and N. J. C. PACKHAM, *Proc. Conf. Cold Fusion Phenomena*, Washington, D.C., October 1989.
28. D. R. ROLISON and W. E. O'GRADY, "Mass/Charge Anomalies in Pd After Electrochemical Loading with Deuterium," *Proc. NSF/EPRI Workshop Anomalous Effects in Deuterated Materials*, Washington, D.C., October 16–18, 1989.
29. R. TANIGUCHI, T. YAMAMOTO, and S. IRIE, "Detection of Charged Particles Emitted by Electrolytically Induced Cold Nuclear Fusion," *Jpn. J. Appl. Phys.*, **28**, 2021 (1989).
30. N. WADA and K. NISHIZAWA, "Nuclear Fusion in Solids," *Jpn. J. Appl. Phys.*, **28**, 2017 (1989).
31. H. O. MENLOVE, M. M. FOWLER, E. GARCIA, A. MAYER, M. C. MILLER, R. R. RYAN, and S. E. JONES,

- "Measurement of Neutron Emission from Ti and Pd in Pressurized D₂ Gas and D₂O Electrolysis Cells," LANL-LAUR:89-1974, Los Alamos National Laboratory (July 27, 1989).
32. R. J. BEUHLER, G. FRIEDLANDER, and L. FRIEDMAN, "Cluster-Impact Fusion," *Phys. Rev. Lett.*, **63**, 1292 (1989).
33. R. C. KAINTHLA, M. SZKLARCZYK, L. KABA, G. H. LIN, O. VELEV, N. J. C. PACKHAM, J. C. WASS, and J. O'M. BOCKRIS, "Eight Chemical Explanations of the Fleischmann-Pons Effects," *Int. J. Hydrogen Energy*, **14**, 771 (1989).
34. F. J. MAYER, J. S. KING, and J. R. REITZ, "Fusion in from the Cold?" *Proc. Workshop Cold Fusion Phenomena*, Santa Fe, New Mexico, May 23-25, 1989.
35. M. GAJDA, D. HARLEY, and J. RAFELSKI, *Proc. Workshop Cold Fusion Phenomena*, Santa Fe, New Mexico, May 23-25, 1989.
36. R. SEITZ, "Fusion in from the Cold?" *Nature*, **339**, 185 (1989).
37. K. NAGAMINE et al., *Proc. Workshop Cold Fusion Phenomena*, Santa Fe, New Mexico, May 23-25, 1989.
38. A. SHYAM, M. SRINIVASAN, S. B. DEGWEKAR, and L. V. KULKARNI, "Multiplicity Distribution of Neutron Emission in Cold Fusion Experiments," in "BARC Studies in Cold Fusion," BARC-1500, Paper A4, Bhabha Atomic Research Centre (1989).
39. B. J. B. CROWLEY, "Nuclear Fusion in High Density Matter," *Nucl. Fusion*, **29**, 2199 (1989).
40. A. J. LEGGETT and G. BAYM, "Can Solid-State Effects Enhance the Cold-Fusion Rate?" *Nature*, **340**, 45 (1989).
41. A. J. LEGGETT and G. BAYM, "Exact Upper Boundary on Barrier Penetration Probabilities in Many-Body Systems: Application to 'Cold Fusion,'" *Phys. Rev. Lett.*, **63**, 191 (1989).
42. C. J. HOROWITZ, "Cold Nuclear Fusion in Metallic Hydrogen and Normal Metals," *Phys. Rev.*, **C40**, R1555 (1989).
43. A. BURROWS, "Enhancement of Cold Fusion in Metal 'Hydrides' by Screening of Proton and Deuteron Charges," *Phys. Rev.*, **B40**, 3405 (1989).
44. Z. SUN and D. TOMANEK, "How Close Can Deuterium Atoms Come Inside Palladium?" *Phys. Rev. Lett.*, **63**, 59 (1989).
45. X. W. WANG, S. G. LOUIE, and M. L. COHEN, "Hydrogen Interactions in PdH_n (1 ≤ n ≤ 4)," *Phys. Rev.*, **B40**, 5822 (1989).
46. C. J. BENESH and J. P. VARY, "Fusion Rates of Squeezed and Screened Hydrogenic Nuclei," *Phys. Rev.*, **C40**, R495 (1989).
47. S. N. VAIDYA and Y. S. MAYYA, "The Role of Combined Electron-Deuteron Screening in d-d Fusion in Metals," in "BARC Studies in Cold Fusion," BARC-1500, Paper C3, Bhabha Atomic Research Centre (1989).
48. S. K. GHOSH, H. K. SADHUKHAN, and A. K. DHARA, "A Theory of Cold Nuclear Fusion in Deuterium Loaded Palladium," in "BARC Studies in Cold Fusion," BARC-1500, Paper C4, Bhabha Atomic Research Centre (1989).
49. T. TAJIMA, H. IYETOMI, and S. ICHIMARU, "Statistical-Mechanical Theory of Cold Nuclear Fusion in Metal Hydrides" (to be published).
50. M. RABINOWITZ and D. H. WORLEDGE, Electric Power Research Institute, Private Communication (Sep. 1989).
51. V. I. GOLDANSKII and F. I. DALIDCHIK, "Mechanism of Solid-State Fusion," *Nature*, **342**, 231 (1989).
52. L. TURNER, "Thoughts Unbottled by Cold Fusion," *Phys. Today*, 140 (Sep. 1989).
53. R. T. BUSH, "A Transmission Resonance Model for Cold Fusion," presented at Annual Mtg. American Society of Mechanical Engineers, San Francisco, California, December 10-15, 1989, paper 89-WA/TS-3.
54. M. DANOS, National Institute of Standards and Technology, Private Communication (June 1989).
55. J. C. JACKSON, "Cold Fusion Results Still Unexplained," *Nature*, **339**, 345 (1989).
56. P. R. BUDELOV, Private Communication (Oct. 1989).
57. M. JANDEL, "Cold Fusion in a Confining Phase of Quantum Electrodynamics," *Fusion Technol.*, **17**, 493 (1990).
58. T. BRESSANI, E. DEL GIUDICE, and G. PREPARATA, "First Steps Toward an Understanding of 'Cold' Nuclear Fusion," *Il Nuovo Cimento*, **101**, 845 (1989).
59. X. L. JIANG, N. XU, and L. J. HAN, "Micropinch in Cold Nuclear Fusion," *Nature* (to be published).
60. G. H. LIN, R. C. KAINTHLA, N. J. C. PACKHAM, and J. O'M. BOCKRIS, "Electrochemical Fusion: A Mechanism Speculation," *J. Electroanal. Chem.* (to be published).
61. J. R. OPPENHEIMER and M. PHILIPS, "Note on the Transmutation Function for Deuterons," *Phys. Rev.*, **48**, 500 (1935).